Fault gouge melting at shallow depth during the 2008 Mw 7.9 Wenchuan earthquake

H. Wang[1,2,3], H.B. Li[1,2,3*], G. Di Toro[4,5], L.-W. Kuo[6], E. Spagnuolo[5], S. Aretusini[5], J.L. Si[1,2.3], S.-R. Song[7]

[1]MNR Key Laboratory of Deep-Earth Dynamics, Institute of Geology, Chinese Academy of Geological Sciences, Beijing 100037, China

[2]Southern Marine Science and Engineering Guangdong Laboratory (Guangzhou), Guangzhou 511458, China

[3]Jiangsu Donghai Continental Deep Hole Crustal Activity National Observation and Research Station, Jiangsu 222300, China

[4]Dipartimento di Geoscienze, Università di Padova, Padova 35131, Italy

[5]Istituto Nazionale di Geofisica e Vulcanologia, Rome 00143, Italy

[6]Department of Earth Sciences, National Central University, Taoyuan 32001, Taiwan

[7]Department of Geosciences, National Taiwan University, Taipei 10617, Taiwan

ABSTRACT

Typical rocks at shallow depths of seismogenic faults are fluid-rich gouges. During earthquakes, on-fault frictional heating may trigger thermal pressurization and dynamic fault weakening. Here we show that frictional melting, rather than thermal pressurization, occurred at shallow depths during the 2008 Mw 7.9 Wenchuan earthquake (WCEQ, China). One year after the WCEQ, we found a ~2-mm-thick glass-bearing pseudotachylyte (solidified frictional melt) in the fault gouges retrieved at 732.6 m depth from the WFSD-1 borehole. The matrix of pseudotachylyte is enriched in barium and cut by barite-bearing veins, evidence of co- and post-

seismic fluid percolation. Because pseudotachylyte can be rapidly altered in the presence of percolating fluids, its preservation suggests that gouge melting occurred in a recent large earthquake, possibly the WCEQ. Rock friction experiments on fluid-rich fault gouges deformed at conditions expected for seismic slip at borehole depths showed the generation of pseudotachylytes. This result, together with the presence at 589.2 m depth of a second slip zone attributed to the WCEQ, implies that during large earthquakes frictional melting can occur at shallow depths and that seismic slip can be accommodated by multiple faults. This conclusion is consistent with the evidence from surface faulting that multiple ruptures propagated during the WCEQ.

INTRODUCTION

The structure of major fault zones includes one or more localized meter-thick fault cores, surrounded by a damage zone cut by a dense network of fractures and minor faults (Faulkner et al., 2010). In the shallow crust, fault cores are commonly composed of fluid-rich gouges (Sibson, 1977; Wibberley et al., 2008). During individual earthquakes, seismic sliding localizes in mm- to cm-thick principal slip zones (PSZ) cutting fault cores (Sibson, 2003). The relative motion of fault wall rocks occurs at average slip rates of ~1 m/s, which results, given the lithostatic load, in frictional heating and thermal expansion of the granular material and the trapped fluid (Rice, 2006; Brantut et al., 2010). Since the thermal expansion of fluid is faster than that of solid components, the unbalance results in fluid pressurization, large coseismic weakening, and buffering of the temperature increase in the slipping zone (Rice, 2006; Brantut et al., 2010). Thus, frictional melting of fluid-rich gouges seems unlikely to occur during seismic faulting at shallow depths. In addition, post-seismic fluid percolation alters the pseudotachylyte (PT) fabrics

due to glass crystallization and dissolution, and mineral precipitation, and may result in rock assemblages similar to those of common fault rocks such as cataclasites and gouges (Kirkpatrick and Rowe, 2013). As a consequence, in fluid-rich faults, the microstructural evidence of gouge melting might be rapidly lost from the geological record (Fondriest et al., 2020).

Here we report the occurrence of PT within fault gouges retrieved from 732.6 m depth from the first borehole of the Wenchuan earthquake Fault Scientific Drilling project (WFSD-1). The presence of PT is documented by focused ion beam–transmission electron microscopy. Rock friction experiments on fault gouges deformed at conditions expected for coseismic slip at borehole depths showed the generation of PT. These field, experimental, and microstructural observations suggest that frictional melting of fluid-rich fault gouges may occur at shallow crustal depths during large earthquakes.

GEOLOGICAL SETTING

The NE-trending Longmen Shan thrust belt is a major structure along the eastern margin of the Tibetan Plateau, which hosted the catastrophic 2008 Wenchuan earthquake (WCEQ, Fig. 1A). To investigate the mechanics of seismic faulting, the WFSD project, including six boreholes along the ruptured Yingxiu-Beichuan (YBF) and the Guanxian-Anxian faults (Fig. 1B), was implemented quickly after the mainshock (Li et al., 2013). The WFSD-1 was drilled along the YBF near Bajiaomiao village (Fig. 1B). During the WCEQ, two seismic ruptures propagated from the south towards the north along the Yingxiu and the nearby Shenxigou faults (Fig. 1A, Fig. S1). The Yingxiu fault ruptured as pure thrust, while the Shenxigou fault was a dextral transpressive fault (Pan et al., 2014). The two faults merged into one approaching the Earth's surface at Bajiaomiao village, where two sets of striae on the fault surface record the propagation

of two ruptures. The fault accommodated vertical and horizontal displacements up to ~6.5 m and ~2.5 m, respectively.

The WFSD-1 cores are composed of the Neoproterozoic Pengguan Magmatic Complex above 585.75 m depth, and of the Late Triassic Xujiahe Formation sedimentary rocks below (Li et al., 2013). Fault rocks at 482-759 m-depth, containing PT, cataclasite, fault breccia, and fault gouge, compose the YBF (Fig. 1C, Wang et al., 2019). The PSZ of the WCEQ was proposed to be located at 589.2 m (PSZ589) within a black fault gouge (Li et al., 2013), where well-crystallized graphite, instead of amorphous carbonaceous materials in the adjacent host rock, was found (Kuo et al., 2014). The graphitization of the carbonaceous minerals was associated with the high-temperature pulse generated during seismic slip (Kuo et al., 2017) and possibly contributed to the very low coseismic fault friction (Li et al., 2015).

NATURAL PSEUDOTACHYLYTE FROM WFSD-1

The drill core studied here retrieved at 732.4-732.8 m-depth on 9 May 2009 (i.e., one year after the WCEQ) is made of sub-parallel layers of > 20-cm-thick coarse-grained and 2-to-3-cm-thick fine-grained fault breccias, a 2-mm-thick fault gouge, and 2-mm-thick glass-like material cut by a lineated fresh-looking mirror-like slip surface (Figs. 1D-E). 14 thin sections were made by this core (SM Note 2). The microstructural investigations of the fault rocks were conducted with optical, scanning (coupled to an energy dispersive spectrometer, FESEM/EDX), and focused ion beam-transmission electron (FIB-TEM: 20-nm rock slices) microscopy. The non-cohesive fine-grained fault breccia contains mainly angular grains of quartz, feldspar, and ankerite, ranging from tens of μm to mm in size. The fault gouge is mainly made of angular to sub-angular quartz and feldspar clasts, as well as an ultrafine matrix with accessory minerals

(Figs. 2A-B, Fig. S3, Table S1). The cohesive glass-like layer is composed of angular to sub-rounded quartz clasts from a few to tens of μm in size (Figs. 2A-B) immersed in a matrix brighter in color than both the fault gouge and the breccia layers (Fig. 2B). The bright color of the glassy matrix is related to enrichment in heavier chemical elements (Fig. 2E, Fig. S4). The matrix is amorphous under the FIB-TEM beam (diffraction pattern with diffuse scattering intensity, Fig. 2F). The amorphous matrix includes 50-to-100-nm-thick, up to 1-μm-long curved ripples resembling flow structures with a slightly different grey intensity color (Fig. 2F), likely associated with minor changes in K-content (TEM-EDX analyses, Figs. 2G-H). The amorphous matrix is cut by a pervasive network of randomly oriented open microcracks spaced < 1 μm apart (Figs. 2C-D) and by a few veins filled with barite (Fig. S5).

ARTIFICIAL PSEUDOTACHYLYTE FROM FRICTION EXPERIMENTS

To verify if fault gouge melting can occur at shallow depth, we conducted rotary-shear friction experiments with SHIVA (Di Toro et al., 2010) at the Istituto Nazionale di Geofisica e Vulcanologia on powdered fault breccias retrieved at 706-732 m-depth in the WFSD-1 borehole. The gouges were sheared up to 5 m and at slip rates of 1 m/s under normal stress of 20 MPa (i.e., lower range of the stress normal to the fault at this depth) under room humidity and fluid-rich (by adding 20 wt.% distilled water) conditions (SM Note 4).

Under room humidity conditions, the friction coefficient μ decayed with slip distance from a peak value of ~0.6-0.7 at slip initiation, to a minimum value of ~0.2 (S1545: rock holders) or 0.45 (S1541, S1543: metal holders) (Fig. 3A). Under fluid-rich conditions, the μ decayed from ~0.6-0.7 at slip initiation to 0.3 (S1547, S1891: metal holders) (Fig. 3B). After the experiment, regardless of the slip distance and the ambient conditions, the sheared gouges contain a bright in

color glass-like layer which includes micro- to nano-vesicles and clasts of quartz with angular to sub-angular shapes (Figs. 3C-F). Vesicles are less abundant and smaller in the gouges sheared under fluid-rich conditions.

DISCUSSION AND CONCLUSIONS

Fault Gouge Melting during the WCEQ

The formation of amorphous material in slip zones may result from ultracomminution or frictional melting (Wenk, 1978; Han et al., 2014). The fault gouges bounding the natural glass-like layer include quartz, feldspar, ankerite, chlorite, and mica (Table S1). The presence of only quartz clasts in the slip zone (Fig. S4) implies that seismic slip activated physical-chemical processes due to shear heating that leads to rock melting (Rice, 2006), mineral dehydration (Brantut et al., 2010) or decomposition (Sulem and Famin, 2009), resulting in the preferential consuming of feldspar, ankerite, chlorite, and mica. Instead, quartz clasts survived, as it has the highest melting point among these minerals (Spray, 2010). The curved ripples in the amorphous matrix may be due to melt migration or derived from the melting of minerals that have been stretched and folded as a result of viscous shearing (Wallace et al., 2019). The mineralogical and microstructural evidence reported above suggests that the glassy layer is the result of solidification of friction melts and thus can be called a PT (Sibson, 1975). Importantly, the PT is associated with a non-cohesive fluid-rich fault gouge.

Previous experiments reproducing the WCEQ deformation conditions but at a shallower depth (Kuo et al., 2014, 2017) or performed on more clay-rich gouges (Kuo et al., 2022) did not result in the production of PT. Instead, the experiments presented here confirm that PT may form

during the WCEQ, also in fluid-rich gouges, but at the larger confining stresses expected at 732 m depth (SM Note 4).

The natural PT is quite similar to the artificial PT produced by shearing fluid-rich gouges (Figs. 3E-F). In the fluid-rich experiments, the presence of water should reduce the temperature of melting resulting in larger amounts of melt produced (Allen, 1979). Moreover, the measured μ is lower when low thermal conductivity holders (S1545, Fig. S7A) are used (e.g., Yao et al., 2016), suggesting that in natural faults under fluid-rich conditions, the μ could be lower than 0.2. Because of the limited amount of gouge available from the borehole, in the experiments we used gouges recovered at 706-732 m-depth, near to the PSZ732. These gouges included 4-12 wt.% of CO_2-bearing minerals (calcite, dolomite, ankerite, etc., Table S1) which breakdown during frictional sliding and release CO_2 which is almost immiscible in silicate-built melts resulting in the formation of vesicles in the artificial PTs (Gomila et al., 2021).

The microcracks in the natural PT are interpreted as resulting from rapid melt solidification and glass contraction, possibly caused by late coseismic to early post-seismic fluid influx. In fact, the natural PT of WFSD-1 was probably produced in a fluid-rich gouge layer, consistently with the evidence of vigorous fluid circulation in the fault zone during the seismic cycle (Xue et al., 2013). However, glass is rarely preserved in natural PTs (Scambelluri et al., 2017) and never found in the very few PTs associated with fault gouges (Otsuki et al., 2009). Most natural PTs are devitrified or altered because the glassy material is unstable under typical geological conditions and especially in the presence of percolating fluids (Kirkpatrick and Rowe, 2013; Fondriest et al., 2020). Therefore, the preservation of glass in the fluid-rich gouges, cut by barite-bearing veins associated with post-seismic fluid percolation, implies that the PT was produced recently, likely during the 2008 WCEQ.

Implications for Seismic Faulting

Geological evidence supports the hypothesis that the glassy PT was produced at very shallow depths in the Earth's crust. The PT is hosted in the Triassic Xujiahe formation, where the exhumation rate is estimated at 0.4-0.65 mm/year (Godard et al., 2009; Wang et al., 2012). Paleoseismic investigations show that large earthquakes occur in the Longmen Shan fault zone with a recurrence interval of about 3000 years (Shen et al., 2009). Assuming uplift and erosion are in balance, the amount of denudation is roughly equivalent to the amount of the rock uplift (Godard et al., 2010), thus the maximum uplift during a large earthquake is ~ 4 m. This is in agreement with GPS measurements of the deformation of 1-2 mm/year accommodated over the entire Longmen Shan area, which is released abruptly in rare but large earthquakes (Zhang, 2013). If the PT formed during the last large seismic event before the WCEQ, the formation depth could be ~736 m, and, if older, the PT should be partially or completely altered over thousands of years (SM Note 5; Fondriest et al., 2020). This reasoning constrains the maximum formation depth of the studied PT to < 1 km. Given that there was no earthquake > M_W 7 in the Longmen Shan fault zone in the past 2700 years (Zhang, 2013), we suggest that the PT at 732.6 m depth is a PSZ (PSZ732) associated with the WCEQ. This conclusion challenges the common hypothesis that PTs are rare and limited to fluid-deficient environments (Sibson and Toy, 2006). The scarcity of PTs within fault zones may be because they are rarely preserved or simply rarely recognized, as their microstructural features are progressively obliterated on geologic time scales by successive faulting, alteration, and devitrification processes.

The WCEQ was characterized by a complex rupture pattern similar to what has been recently observed from the Kaikoura 2016 Mw 7.8 earthquake in New Zealand (Hamling et al., 2017). Two coseismic surface rupture zones merged into one at the Bajiaomiao village (Fig. S1)

where a single fault surface with two coseismic striations (thrust- and transpressive-related) is exposed (Fig. 4B). This field evidence is consistent with the finding of two PSZs at depths in WFSD-1 which merged towards the Earth's surface (Fig. 4). As a consequence, during its complex rupture, the WCEQ activated different on-fault processes in nearby fault zone volumes (Fig. 4A), including coseismic gouge graphitization in the PSZ589 (Fig. 4C), and frictional melting of fluid-rich gouges (Fig. 4D) at larger, but still shallow, depth.

ACKNOWLEDGMENTS

The authors thank the three anonymous reviewers, their comments and suggestions helped to improve the quality of the manuscript. This research was supported by the National Natural Science Foundation of China (grants 41830217 and 41972229), Key Special Project for Introduced Talents Team of Southern Marine Science and Engineering Guangdong Laboratory (Guangzhou) (grant GML2019ZD0201), and the European Research Council CoG project 614705 NOFEAR. C. Janssen and R. Wirth are acknowledged for their assistance with FIB-TEM imaging; F. Zorzi and M. Favero are thanked for the X-ray powder diffraction analysis.

REFERENCES CITED

Allen, A.R., 1979, Mechanism of frictional fusion in fault zones: Journal of Structural Geology, v. 1, p. 231-243.

Brantut, N., Schubnel, A., Corvisier, J., and Sarout, J., 2010, Thermochemical pressurization of faults during coseismic slip: Journal of Geophysical Research: Solid Earth, v. 115, B05134, https://doi.org/10.1029/2009JB006533.

Di Toro, G., Niemeijer, A., Tripoli, A., Nielsen, S., Di Felice, F., Scarlato, P., Spada, G.,

Alessandroni, R., Romeo, G., Di Stefano, G., Smith, S., Spagnuolo, E., and Mariano, S., 2010, From field geology to earthquake simulation: a new state-of-the-art tool to investigate rock friction during the seismic cycle (SHIVA): Rendiconti Lincei. Scienze Fisiche e Naturali, v. 21, p. 95–114, https://doi.org/10.1007/s12210-010-0097-x.

Faulkner, D.R., Jackson, C.A.L., Lunn, R.J., Schlische, R.W., Shipton, Z.K., Wibberley, C.A.J., and Withjack, M.O., 2010, A review of recent developments concerning the structure, mechanics and fluid flow properties of fault zones: Journal of Structural Geology, v. 32, p. 1557–1575, https://doi.org/10.1016/j.jsg.2010.06.009.

Fondriest, M., Mecklenburgh, J., Passelegue, F.X., Artioli, G., Nestola, F., Spagnuolo, E., Rempe, M., and Di Toro, G., 2020, Pseudotachylyte alteration and the rapid fade of earthquake scars from the geological record: Geophysical Research Letters, v. 47, p. 1–9 https://doi.org/10.1029/2020GL090020.

Godard, V., Pik, R., Lavé, J., Cattin, R., Tibari, B., de Sigoyer, J., Pubellier, M., and Zhu, J., 2009, Late Cenozoic evolution of the central Longmen Shan, eastern Tibet: Insight from (U-Th)/He thermochronometry: Tectonics, v. 28, TC5009, https://doi.org/10.1029/2008TC002407.

Godard, V., Lavé, J., Carcaillet, J., Cattin, R., Bourlès, D., and Zhu, J., 2010, Spatial distribution of denudation in Eastern Tibet and regressive erosion of plateau margins: Tectonophysics, v. 492, p. 253–274, https://doi.org/10.1016/j.tecto.2009.10.026.

Gomila, R., Fondriest, M., Jensen, E., Spagnuolo, E., Masoch, S., Mitchell, T.M., Magnarini, G., Bistacchi, A., Mittempergher, S., Faulkner, D., Cembrano, J., and Di Toro, G., 2021, Frictional melting in hydrothermal fluid–rich faults: Field and experimental evidence from the Bolfín Fault Zone (Chile): Geochemistry, Geophysics, Geosystems, v. 22,

e2021GC009743, https://doi.org/10.1029/2021GC009743.

Hamling, I.J., Hreinsdottir, S., Clark, K., Elliott, J., Liang, C., Fielding, E., Litchfield, N., Villamor, P., Wallace, L., Wright, T., D'Anastasio, E., Bannister, S., Burbidge, D., Denys, P., Gentle, P., Howarth, J., Mueller, C., Palmer, N., Pearson, C., and Stirling, M., 2017, Complex multifault rupture during the 2016 MW7.8 Kaikōura earthquake, New Zealand: Science, v. 356, eaam7194, https://doi.org/10.1126/science.aam7194.

Han, R., Hirose, T., Jeong, G.Y., Ando, J., and Mukoyoshi, H., 2014, Frictional melting of clayey gouge during seismic fault slip: Experimental observation and implications: Geophysical Research Letters, v. 41, p. 5457–5466, https://doi.org/10.1002/2014GL061246.

Kirkpatrick, J.D., and Rowe, C.D., 2013, Disappearing ink: how pseudotachylytes are lost from the rock record: Journal of Structural Geology, v. 52, p. 183–198, https://doi.org/10.1016/j.jsg.2013.03.003.

Kuo, L.W., Di Felice, F., Spagnuolo, E., Di Toro, G., Song, S.R., Aretusini, S., Li, H.B., Suppe, J., Si, J.L., and Wen C.Y., 2017, Fault gouge graphitization as evidence of past seismic slip: Geology, v. 45, p. 979–982, https://doi.org/10.1130/G39295.1.

Kuo, L.W., Li, H.B., Smith, S.A.F., Di Toro, G., Suppe, J., Song, S.R., Nielsen, S., Sheu, H.S., and Si, J.L., 2014, Gouge graphitization and dynamic fault weakening during the 2008 Mw 7.9 Wenchuan earthquake: Geology v. 42, p. 47–50, https://doi.org/10.1130/G34862.1.

Kuo, L.W., Hung, C.C., Li, H., Aretusini, S., Chen, J., Di Toro, G., Spagnuolo, E., Di Felice, F., Wang, H, Si, J.L., and Sheu, H.S., 2022, Frictional properties ofthe Longmenshan fault belt gouges from WFSD-3 and implications for earthquake rupture propagation: Journal of Geophysical Research: Solid Earth, v. 127, e2022JB024081, https://doi.org/10.1029/2022JB024081.

Li, H.B., Wang, H., Xu, Z.Q., Si, J.L., Pei, J.L., Li, T.F., Huang, Y., Song, S.R., Kuo, L.W., Sun, Z.M., Chevalier, M.L., and Liu, D.L., 2013, Characteristics of the fault-related rocks, fault zones and the principal slip zone in the Wenchuan Earthquake Fault Scientific Drilling Project Hole-1 (WFSD-1): Tectonophysics, v. 584, p. 23–42, https://doi.org/10.1016/j.tecto.2012.08.021.

Li, H.B., Xue, L., Brodsky, E.E., Mori, J.J., Fulton, P.M., Wang, H., Kano, Y., Yun, K., Harris, R.N., Gong, Z., Li, C.L., Si, J.L., Sun, Z.M., Pei, J.L., Zheng, Y., and Xu, Z.Q., 2015, Long-term temperature records following the Mw 7.9 Wenchuan (China) earthquake consistent with low friction: Geology, v. 43, p. 163–166, https://doi.org/10.1130/G35515.1.

Otsuki, K., Hirono, T., Omori, M., Sakaguchi, M., Tanigawa, W., Lin, W.R., and Song, S.R., 2009, Analyses of pseudotachylyte from Hole-B of Taiwan Chelungpu Fault Drilling Project (TCDP); their implications for seismic slip behaviors during the 1999 Chi-Chi earthquake: Tectonophysics, v. 469, p. 13–24, https://doi.org/10.1016/j.tecto.2009.01.008.

Pan, J.W., Li, H.B., Si, J.L., Pei, J.L., Fu, X.F., Chevalier, M.L., and Liu, D.L., 2014, Rupture process of the Wenchuan earthquake (Mw 7.9) from surface ruptures and fault striations characteristics: Tectonophysics, v. 619–620, p. 13–28, https://doi.org/10.1016/j.tecto.2013.06.028.

Rice, J.R., 2006, Heating and weakening of faults during earthquake slip: Journal of Geophysical Research: Solid Earth, v. 111, p. 1–29, https://doi.org/10.1029/2005JB004006.

Scambelluri, M., Pennacchioni, G., Gilio, M., Bestmann, M., Plümper, O., and Nestola, F., 2017, Fossil intermediate-depth earthquakes in subducting slabs linked to differential stress release: Nature Geosciences, v. 10, p. 960–966, https://doi.org/10.1038/s41561-017-0010-7.

Shen, Z.K., Sun, J.B., Zhang, P.Z., Wan, Y.G., Wang, M., Bürgmann, R., Zeng, Y.H., Gan, W.J.,

Liao, H., and Wang, Q.L., 2009, Slip maxima at fault junction and rupturing of barriers during the 2008 Wenchuan earthquake: Nature Geosciences, v. 2, p. 718–724, https://doi.org/10.1038/ngeo636.

Sibson, R.H., 1977, Fault rocks and fault mechanisms: Journal of the Geological Society, v. 133, p. 191–213, https://doi.org/10.1144/gsjgs.133.3.0191.

Sibson, R.H., 1975, Generation of pseudotachylyte by ancient seismic faulting: Geophysical Journal International, v. 43, p. 775–794, https://doi.org/10.1111/j.1365-246X.1975.tb06195.x.

Sibson, R.H., 2003, Thickness of the seismic slip zone: Bulletin of the Seismological Society of America, v. 93, p. 1169–1178, https://doi.org/10.1785/0120020061.

Sibson, R.H., and Toy, V., 2006, The habitat of fault-generated pseudotachylyte: presence vs. absence of friction melt, In *Radiated Energy and the Physics of Faulting*, *Geophysical Monograph Series v. 170*, edited by. Abercrombie, R., A. McGarr., G. Di Toro and H. Kanamori, p. 153-166, AGU, Washington, D.C., USA., 2006.

Spray, J.G., 2010, Frictional melting processes in planetary materials: from hypervelocity impact to earthquakes: Annual Review of Earth and Planetary Sciences, v. 38, p. 221–254, https://doi.org/10.1146/annurev.earth.031208.100045.

Sulem, J., and Famin, V., 2009, Thermal decomposition of carbonates in fault zones: slip-weakening and temperature-limiting effects, Journal of Geophysical Research: Solid Earth, v. 114, B03309, https://doi.org/10.1029/2008JB006004.

Wallace, P.A., De Angelis, S.H., Hornby, A.J., Kendrick, J.E., Clesham, S., von Aulock, F.W., Hughes, A., Utley, J.EP., Hirose, T., Dingwell, D.B., and Lavallée, Y., 2019, Frictional melt homogenisation during fault slip: Geochemical, textural and rheological fingerprints:

298 Geochimica et Cosmochimica Acta, v. 255, p. 265–288,
299 https://doi.org/10.1016/j.gca.2019.04.010.
300 Wang, E.Q., Kirby, E., Furlong, K.P., van Soest, M., Xu, G., Shi, X., Kamp, P.J.J., and Hodges,
301 K.V., 2012, Two-phase growth of high topography in eastern Tibet during the Cenozoic:
302 Nature Geosciences, v. 5, p. 640–645, https://doi.org/10.1038/ngeo1538.
303 Wang, H., Li, H.B., Zhang, L., Zheng, Y., Si, J.L., and Sun, Z.M., 2019, Paleoseismic slip
304 records and uplift of the Longmen Shan, eastern Tibetan Plateau: Tectonics, v.38, p. 354–
305 373, https://doi.org/10.1029/2018TC005278.
306 Wenk, H.R., 1978, Are pseudotachylites products of fracture or fusion?: Geology, v. 6, p. 507–
307 511, https://doi.org/10.1130/0091-7613(1978)6<507:APPOFO>2.0.CO;2.
308 Wibberley, C.A.J., Yielding, G., and Di Toro, G., 2008, Recent advances in the understanding of
309 fault zone internal structure: a review: in Wibberley, C.A.J., Kurz, W., Imber, J.,
310 Holdsworth, R.E., Collttttini, C. (eds) the internal structure of fault zones: Implications for
311 mechanical and fluid-flow properites. v.299, p.5-33, https://doi.org/10.1144/SP299.2.
312 Xue, L., Li, H.B., Brodsky, E.E., Xu, Z.Q., Kano, Y., Wang, H., Mori, J.J., Si, J.L., Pei, J.L.,
313 Zhang, W., Yang, G., Sun, Z.M., and Huang, Y., 2013, Continuous permeability
314 measurements record healing inside the Wenchuan earthquake fault zone: Science, v. 340, p.
315 1555–1559, https://doi.org/10.1126/science.1237237.
316 Yao, L., Ma, S.L., Platt, J.D., Niemeijer, A.R., and Shimamoto, T., 2016, The crucial role of
317 temperature in high-velocity weakening of faults: Experiments on gouge using host blocks
318 with different thermal conductivities: Geology, v. 44, p. 63–66,
319 https://doi.org/10.1130/G37310.1.
320 Zhang, P.Z., 2013, Beware of slowly slipping faults: Nature Geosciences, v. 6, p. 232–234

321 https://doi.org/10.1038/ngeo1811.

FIGURE CAPTIONS

Figure 1. Tectonic setting and fault rocks in the WFSD-1 core. A: Active faults in the Tibetan Plateau. B: Tectonic sketch of the Longmen Shan area, and the WFSD drilling sites. F1: Wenchuan-Maoxian fault, F2: Yingxiu-Beichuan fault, F3: Guanxian-Anxian fault. C: Fault rocks in the WFSD-1 core. D: The core at 732.4-732.8 m depth, including a black 2-mm-thick layer bounded by a striated mirror-like principal slip surface (E).

Figure 2. Microstructures of the fault rocks at 732.6 m depth. A-B: The slip zone consists of layers of fault breccia, fault gouge, and glass-like materials. C: The glass-like layer is made of sub-rounded to angular quartz clasts immersed in a light grey matrix. D: The matrix includes randomly oriented open microcracks. E: SEM-EDX spectrum of the spot 1 in image D. F: Glass-like matrix with few tens of nm-thick ripples and microcracks (TEM image). Insert shown the diffraction patterns. G-H: TEM-EDX spectra of areas 2 and 3 in image F. Ga and Cu are from the sample preparation by FIB and the TEM sample holder, respectively. A: optical microscope image, parallel Nicols; B-D: BSE-SEM images.

Figure 3. Experimental data and microstructures (BSE-SEM images) of the sheared gouges. A: Friction coefficient vs. slip under room humidity conditions (S1541 & S1543: metal holders; S1545: rock holder). B: Friction coefficient vs. slip under fluid-rich conditions (metal holders). Curve colored in light gray: gouge extrusion. C: PT produced in S1541. D: PT produced in S1547. E: Close-up view of the PT of S1541: The glass includes numerous vesicles and wraps

344 rounded quartz clasts. F: Close-up view of the PT of S1547: Compared to S1541, the vesicles are
345 smaller and less abundant, and the quartz clasts are more angular.
346
347 Figure 4. Two PSZs of the WCEQ in the WFSD-1 core. A: Geological cross-section across the
348 WFSD-1 (modified from Li et al., 2013). B: Surface rupture near the WFSD-1 drill site. Two sets
349 of striae decorate the fault surface. C: The drill core from 589.04-589.34 m depth includes the
350 graphite-rich PSZ589. D: The drill core from 732.40-732.80 m depth includes the PT-bearing
351 PSZ732.
352
353 [1]Supplemental Material. *[Additional information about the surface rupture zones, sample*
354 *collection and preparation, compositions of the fault rocks, friction experiments, and dissolution*
355 *simulation of the pseudotachylyte.]* Please visit https://doi.org/10.1130/XXXX to access the
356 supplemental material, and contact editing@geosociety.org with any questions.

Figure 1

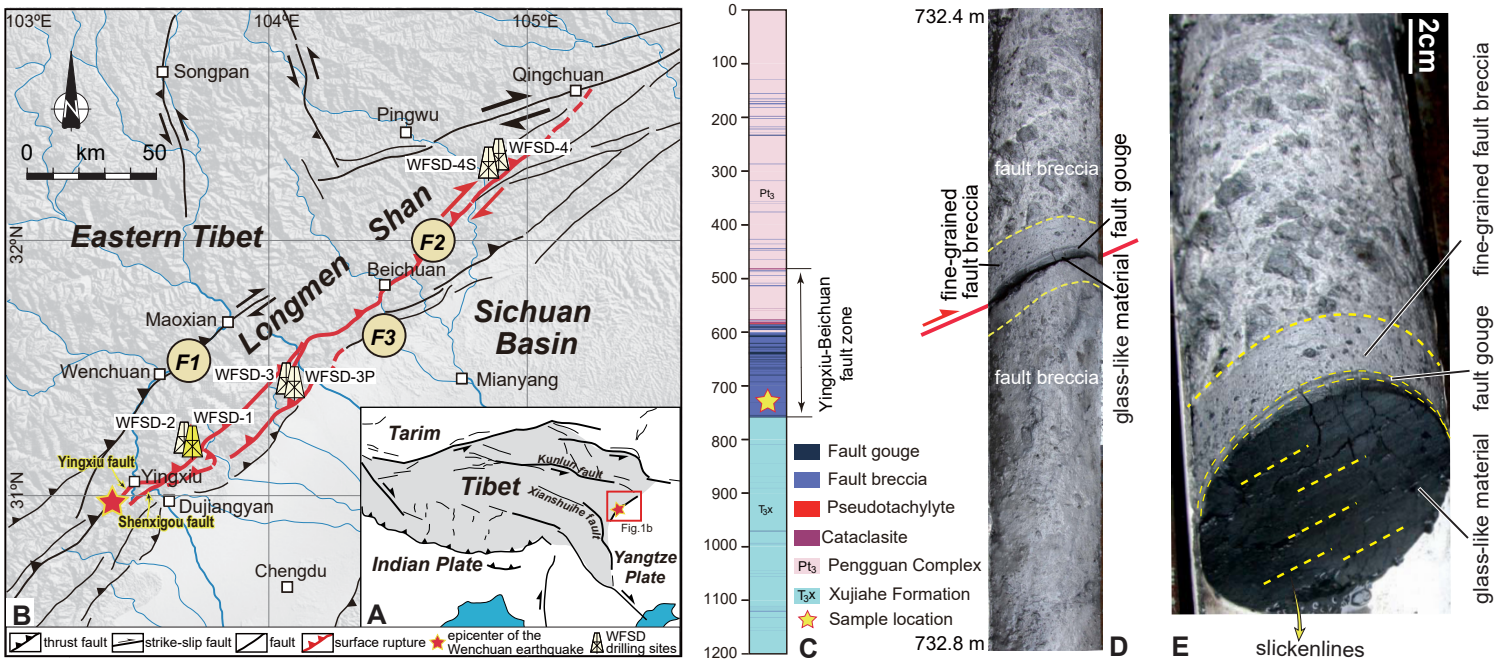
103ºE
104ºE
105ºE
32ºN
31ºN
0 km 50
Songpan
Qingchuan
Pingwu
WFSD-4
WFSD-4S
Eastern Tibet
Shan
Longmen
F2
Beichuan
Maoxian
F1
F3
Sichuan Basin
Wenchuan
WFSD-3
WFSD-3P
Mianyang
WFSD-2
WFSD-1
Yingxiu fault
Yingxiu
Dujiangyan
Shenxigou fault
Chengdu
B
Tarim
Kunlun fault
Tibet
Xianshuihe fault
Fig.1b
Indian Plate
Yangtze Plate
A
thrust fault
strike-slip fault
fault
surface rupture
epicenter of the Wenchuan earthquake
WFSD drilling sites
0
100
200
300
400
500
600
700
800
900
1000
1100
1200
Pt3
T3x
Yingxiu-Beichuan fault zone
Fault gouge
Fault breccia
Pseudotachylyte
Cataclasite
Pengguan Complex
Xujiahe Formation
Sample location
C
732.4 m
732.8 m
fault breccia
fine-grained fault breccia
fault gouge
glass-like material
fault breccia
D
2cm
fine-grained fault breccia
fault gouge
glass-like material
slickenlines
E

Figure 2

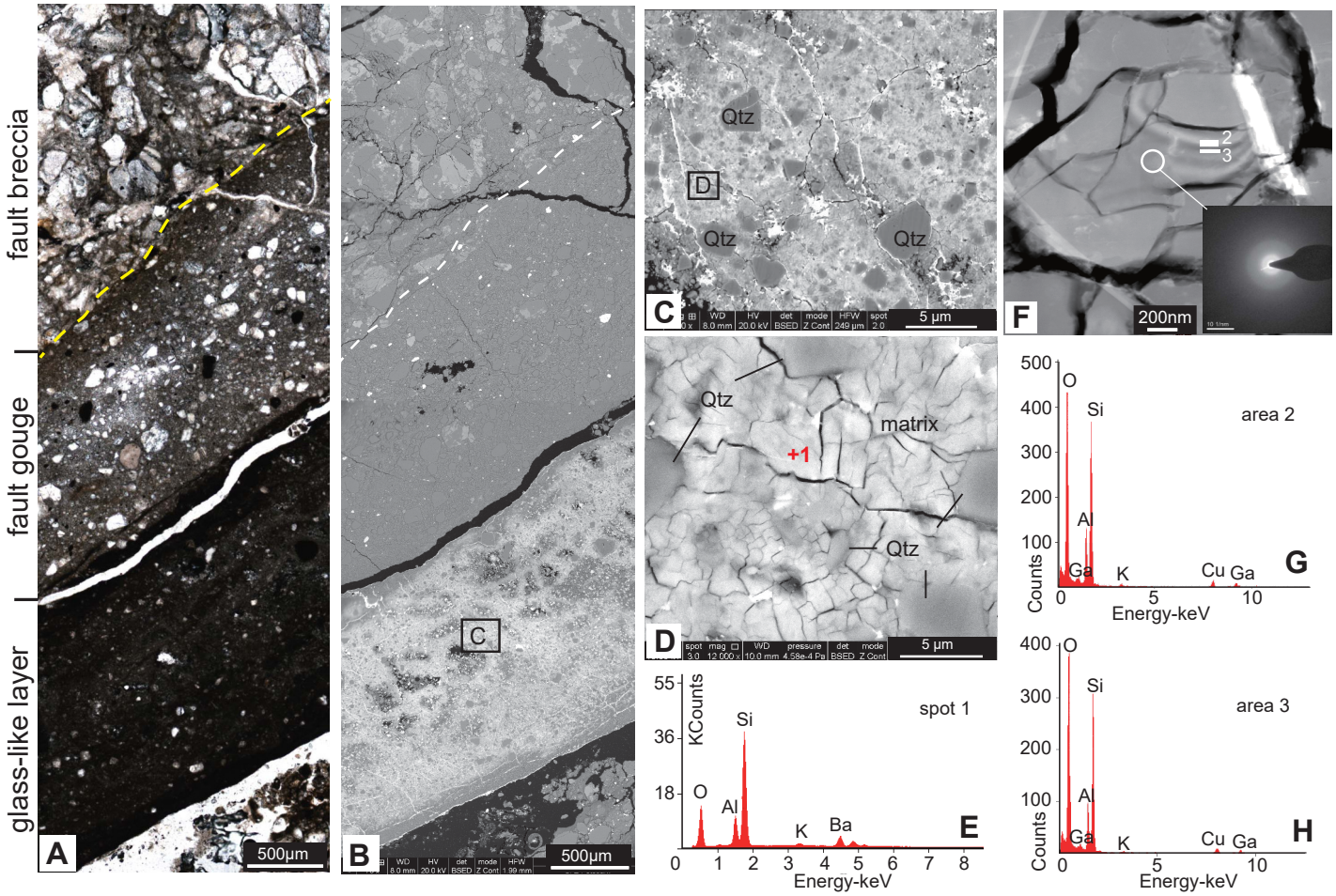
fault breccia
fault gouge
glass-like layer
A
500μm
B
C
500μm
Qtz
D
Qtz
Qtz
C
5 μm
Qtz
matrix
+1
Qtz
D
5 μm
55
36
18
KCounts
O
Si
Al
K
Ba
spot 1
E
0 1 2 3 4 5 6 7 8
Energy-keV
F
2
3
200nm
500
400
300
200
100
Counts
O
Si
Al
Ga
K
Cu Ga
area 2
G
0 5 10
Energy-keV
400
300
200
100
Counts
O
Si
Al
Ga
K
Cu Ga
area 3
H
0 5 10
Energy-keV

Figure 3

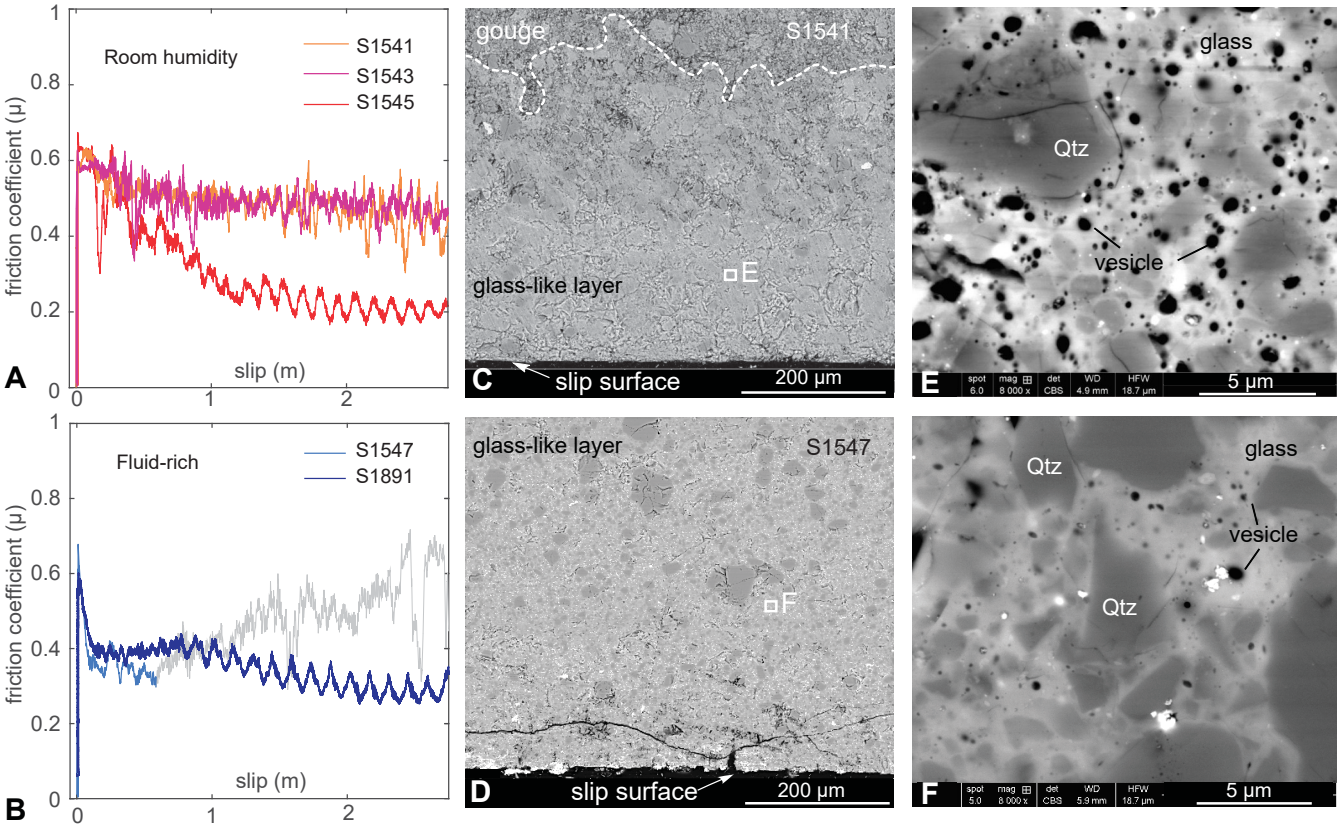
A
Room humidity
S1541
S1543
S1545
friction coefficient (μ)
slip (m)
B
Fluid-rich
S1547
S1891
friction coefficient (μ)
slip (m)
C
gouge
S1541
glass-like layer
E
slip surface
200 μm
D
glass-like layer
S1547
F
slip surface
200 μm
E
glass
Qtz
vesicle
5 μm
F
Qtz
glass
vesicle
Qtz
5 μm

Figure 4

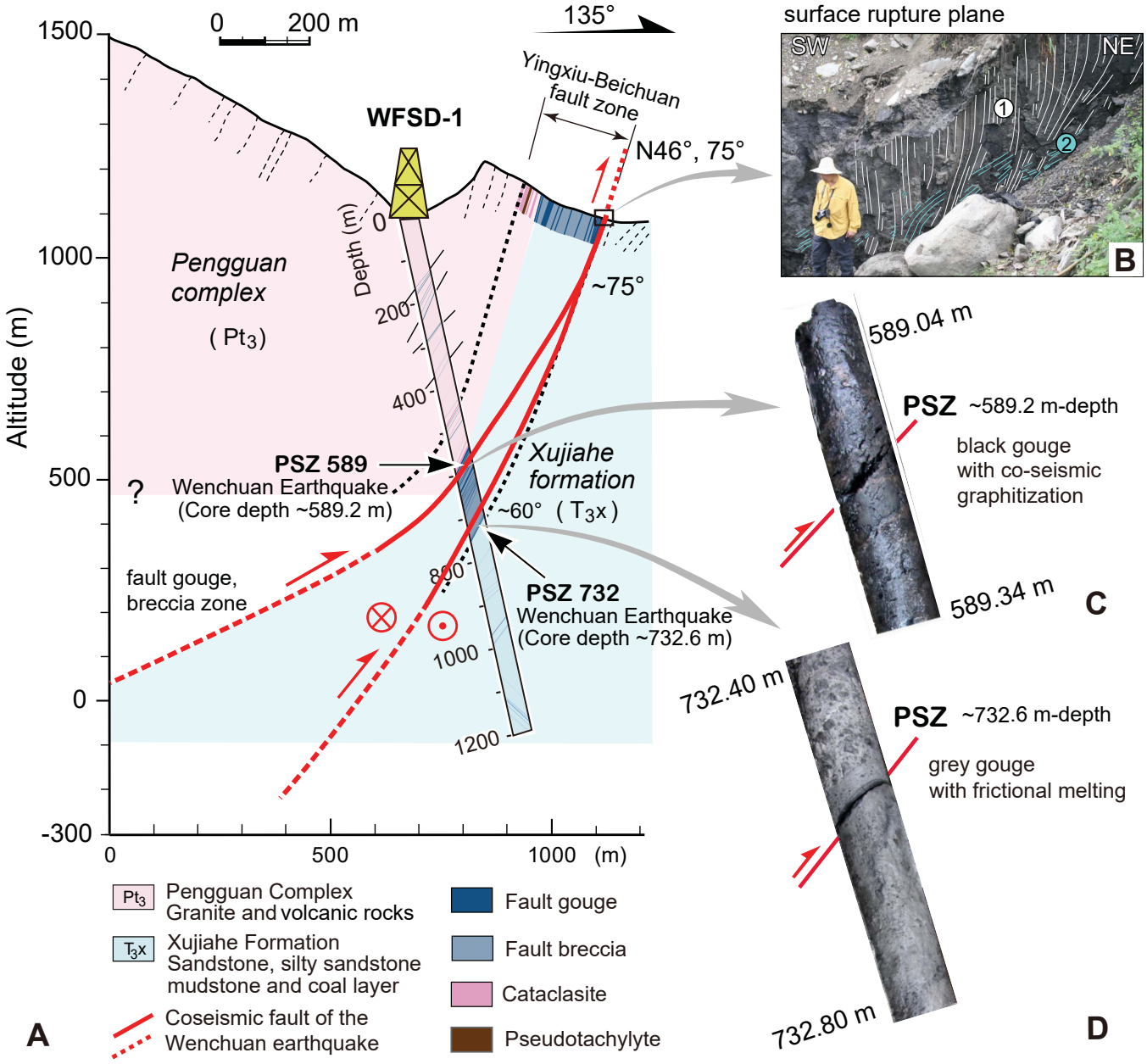
0 200 m
135°
Yingxiu-Beichuan fault zone
WFSD-1
N46°, 75°
surface rupture plane
SW
NE
1
2
B
1500
1000
500
0
-300
Altitude (m)
Depth (m)
0
200
400
600
1000
1200
~75°
Pengguan complex
(Pt3)
PSZ 589
Wenchuan Earthquake
(Core depth ~589.2 m)
?
Xujiahe formation
~60° (T3x)
fault gouge,
breccia zone
PSZ 732
Wenchuan Earthquake
(Core depth ~732.6 m)
589.04 m
PSZ ~589.2 m-depth
black gouge
with co-seismic
graphitization
589.34 m
C
732.40 m
PSZ ~732.6 m-depth
grey gouge
with frictional melting
732.80 m
D
0
500
1000 (m)
Pt3 Pengguan Complex
Granite and volcanic rocks
T3x Xujiahe Formation
Sandstone, silty sandstone
mudstone and coal layer
Coseismic fault of the
Wenchuan earthquake
Fault gouge
Fault breccia
Cataclasite
Pseudotachylyte
A